Immunity
Article

Lymphotoxin-Dependent Prion Replication in Inflammatory Stromal Cells of Granulomas

Mathias Heikenwalder,[1] Michael O. Kurrer,[2,5] Ilan Margalith,[1,5] Jan Kranich,[1,5] Nicolas Zeller,[1,6] Johannes Haybaeck,[1] Magdalini Polymenidou,[1] Matthias Matter,[1] Juliane Bremer,[1] Walker S. Jackson,[3] Susan Lindquist,[3,4] Christina J. Sigurdson,[1] and Adriano Aguzzi[1,*]

[1]Institute of Neuropathology, Department of Pathology, University Hospital of Zurich, Schmelzbergstrasse 12, CH-8091 Zurich, Switzerland
[2]Department of Pathology, Kantonsspital Aarau, Tellstrasse, Aarau, CH-5001, Switzerland
[3]Whitehead Institute for Biomedical Research, 9 Cambridge Center, Cambridge, MA 02142, USA
[4]Howard Hughes Medical Institute, Massachusetts Institute of Technology, Cambridge, MA 02142, USA
[5]These authors contributed equally to this work
[6]Present address: Department of Neuropathology, University of Freiburg, Freiburg, Germany
*Correspondence: adriano.aguzzi@usz.ch
DOI 10.1016/j.immuni.2008.10.014

SUMMARY

Prior to invading the nervous system, prions frequently colonize lymphoid organs and sites of inflammatory lymphoneogenesis, where they colocalize with Mfge8$^+$ follicular dendritic cells (FDCs). Here, we report that soft-tissue granulomas, a frequent feature of chronic inflammation, expressed the cellular prion protein (PrP^C, encoded by *Prnp*) and the lymphotoxin receptor (LTβR), even though they lacked FDCs and did not display lymphoneogenesis. After intraperitoneal prion inoculation, granulomas of *Prnp*$^{+/+}$ mice, but not *Prnp*$^{-/-}$ granulomas or unaffected *Prnp*$^{+/+}$ skin, accumulated prion infectivity and disease-associated prion protein. Bone-marrow transfers between *Prnp*$^{+/+}$ and *Prnp*$^{-/-}$ mice and administration of lymphotoxin signaling antagonists indicated that prion replication required radioresistant PrP^C-expressing cells and LTβR signaling. Granulomatous PrP^C was mainly expressed by stromal LTβR$^+$ mesenchymal cells that were absent from unaffected subcutis. Hence, granulomas can act as clinically silent reservoirs of prion infectivity. Furthermore, lymphotoxin-dependent prion replication can occur in inflammatory stromal cells that are distinct from FDCs.

INTRODUCTION

Transmissible spongiform encephalopathies (TSEs) are infectious neurodegenerative disorders of humans and animals caused by unconventional pathogens termed prions (Aguzzi and Polymenidou, 2004). Throughout this paper, we refer to the "prion" as the infectious agent causing TSEs, without implying that it consists of any specific biophysical entity. Accordingly, prion infectivity is measured by microbiological bioassays and expressed as titer of LD_{50} and ID_{50} units in vivo and in vitro, respectively (Aguzzi and Weissmann, 1997).

PrP^{Sc}, an aggregated, partially proteinase-K (PK) resistant isoform of the cellular host prion protein PrP^C, accumulates in infected organisms and may represent the disease-associated prion (Legname et al., 2004). PrP^C is required as a substrate for prion replication and disease development, and *Prnp*$^{-/-}$ mice lacking PrP^C are resistant to prion infections (Büeler et al., 1993) and to PrP^{Sc} neurotoxicity (Brandner et al., 1996).

Although TSEs selectively damage the CNS, extraneural PrP^C is needed for prion transport from peripheral sites to the CNS (Blättler et al., 1997), and in most TSEs, PrP^{Sc} is detectable in lymphoid organs long before clinical signs (Fraser and Dickinson, 1970; Glatzel et al., 2003). In addition to PrP^C (Büeler et al., 1993), splenic prion replication requires follicular dendritic cells (FDCs) whose maintenance crucially depends on B cells expressing tumor necrosis factor (TNF) and lymphotoxin α (LTα) and LTβ (Prinz et al., 2003). Accordingly, genetic ablation of LT or TNF receptors antagonizes peripheral prion replication (Mabbott et al., 2002; Prinz et al., 2002), and B cell-deficient mice lacking FDCs are resistant to peripheral prion administration (Klein et al., 1997; Klein et al., 1998; Montrasio et al., 2001). Suppression of LTβ receptor (LTβR) signaling by administration of soluble dimeric LTβR (LTβR-Fc) dedifferentiates mature FDCs and impairs peripheral prion pathogenesis (Mabbott et al., 2000; Mabbott et al., 2003; Montrasio et al., 2000).

Certain chronic inflammatory and neoplastic conditions (Hamir et al., 2006; Heikenwalder et al., 2005; Ligios et al., 2005) enable local PrP^{Sc} deposition and prion replication and also display extravasation of B cells and ectopic maturation of FDCs, supporting the idea that FDCs are the primary site of extraneural prion replication. However, not all extraneural prion deposition depends on FDCs. Myocytes and fibroblasts replicate prions in vitro (Dlakic et al., 2007; Mahal et al., 2007; Vorberg et al., 2004) and possibly in vivo (Andreoletti et al., 2004), suggesting that replication is not restricted to immune and neuroectodermal cells. PrP^{Sc} was found in many nonlymphoid sites of patients with Creutzfeldt-Jakob disease and of animals with TSEs (Glatzel et al., 2003; Mathiason et al., 2006; Vascellari et al., 2007). Finally, prion replication can occur in lymph nodes of TNF receptor 1 (TNFR1)-deficient mice that lack FDCs (Oldstone et al., 2002; Prinz et al., 2002). The cells replicating prions in this context have not been characterized.

Thus, there are considerable uncertainties on the nature of the cells replicating prions in extraneural compartments. Here, we

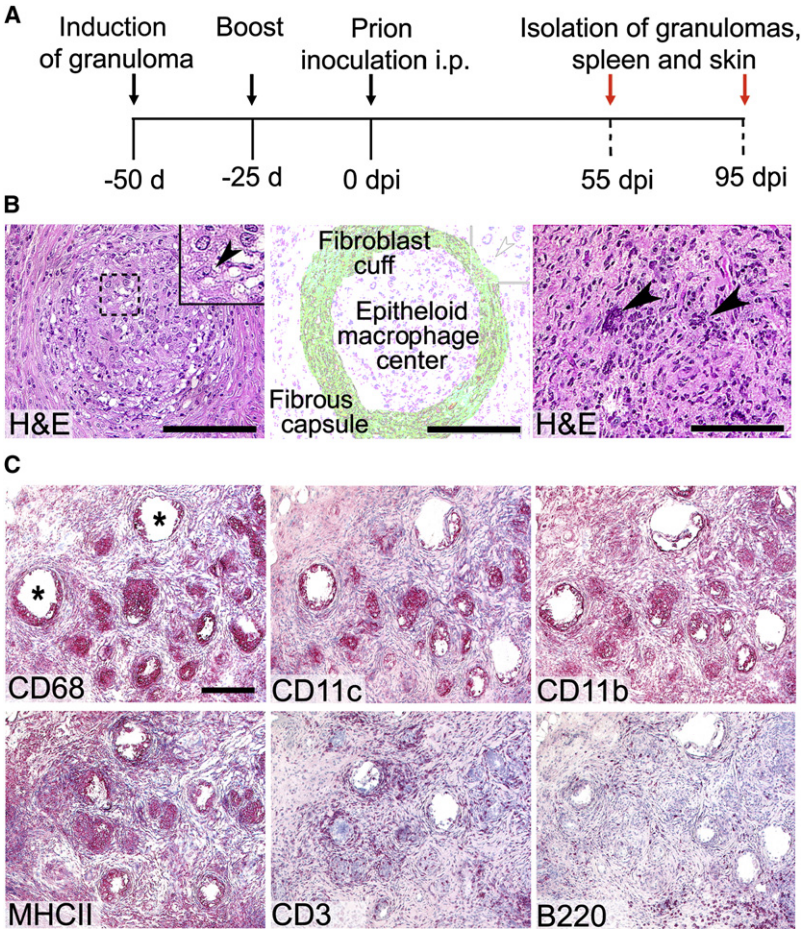

Figure 1. Generation, Prion Inoculation, and Histological Analysis of Granulomas

(A) Time line of granuloma generation, prion inoculation, and organ collection. "Dpi" refers to days after inoculation.

(B) The left panel shows hematoxylin and eosin (H&E) staining of a representative granuloma nodule. The dotted area and inset show detail of an epitheloid macrophage (indicated by an arrowhead). The scale bar represents 150 μm. The center panel shows the scheme of the granuloma depicted on the left, with delineation of the various components. The right panel shows detail of granuloma with multinucleated giant cells (indicated by arrowheads), collagen bundles (reddish streaks), and fibroblasts (elongated cells). The scale bar represents 100 μm.

(C) Immunohistological characterization of granuloma nodules at 55 dpi. CD68, CD11c, and CD11b stains were performed to detect macrophages and epitheloid cells. CD3 and B220 stains were used for detecting T and B lymphocytes, respectively. Asterisks indicate lipid vacuoles. The scale bar represents 250 μm.

investigated conditions in which immune cells would focally accumulate at sites of inflammation, yet no FDCs would be induced. Granulomas fulfill these criteria because they consist mainly of specialized macrophages surrounded by fibroblasts and lymphocytes. Granulomas are highly prevalent in humans and farm animals and can develop at any site of the body in diseases of disparate etiology (Kumar et al., 2004). PrP^C was enriched in mesenchymal $CD45^-LT\beta R^+$ cells within granulomas, with concentrations similar to lymphoid tissue. $Prnp^{+/+}$ granulomas were rapidly colonized by prions. Despite the absence of FDCs, suppression of lymphotoxin signaling reduced the prion load of granulomas. Therefore, a select population of inflammatory stromal cells of granulomas can replicate prions upon LTβR signaling.

RESULTS

Induction and Characterization of Granulomas

Granulomas were induced subcutaneously (s.c.) at two symmetric abdominal sites in $Prnp^{+/+}$, $Prnp^{-/-}$ mice and in *tga20* mice (all C57BL/6x129Sv hybrids) overexpressing PrP^C under the control of the *Prnp* promoter (Fischer et al., 1996) by injection of complete Freund's adjuvans (CFA) or Zymosan resuspended in paraffin oil (Z/PFO). Twenty-five days before prion inoculation (−25 d), granulomas were boosted by reinjection of the inducer mix at the primary injection sites (Figure 1A). This reliably induced granulomas in all mice and ensured granuloma maintenance for at least 145 days. The diameter of granuloma nodules ranged between 1 and 10 mm at 145 days after granuloma induction ("dpgi"). At 50 dpgi mice were inoculated intraperitoneally (i.p.) with prions (strain RML5; 5 $logLD_{50}$ in 100 μl). Granulomas were dissected at 55 or 95 days after prion inoculation ("dpi") and displayed at each time point the characteristic cellular composition and morphology of granulomas (Figure 1 and Figures S1, S2, and S3 available online).

Z/PFO induced accumulations of foamy macrophages with degenerating neutrophils (Figure S2A). In contrast, CFA-induced granulomas closely resembled their human counterparts with central pockets of lipid vacuoles, epitheloid macrophages (Figure 1B, left, arrowhead), multinucleated giant cells (Figure 1B, right arrowheads), neovascularization, and fibrous capsules (Figure 1B). Therefore, further analyses focused on CFA-induced granulomas. Granulomas contained predominantly $CD68^+CD11c^+CD11b^+MHC\text{-}II^+$ cells, most of which were negative for the pan-dendritic cell marker NLDC (Figure S1D) and therefore classified as macrophages (Ordway et al., 2005). Granulomas also contained few $Ly6G^+$ granulocytes (Figure S1B), as well as scattered $CD3^+$ and $B220^+CD19^+$ cells (Figure 1D and Figure S1A).

Larger $B220^+$ cell aggregates were visible at the outer rim of the inflammatory foci (Figure S1B). These aggregates were negative for FDC-M1, CD35, C1qa and FDC-M2 (Figure S1B), suggesting the absence of FDCs. This was further investigated by real-time PCR analysis for the FDC-M1 antigen, Mfge8 (Kranich et al., 2008). *Mfge8* mRNA content of granulomas was indistinguishable from that of $Mfge8^{-/-}$ spleens, or $Lt\beta r^{-/-}$ spleens (Figure S1C), confirming that granulomas were devoid of FDCs.

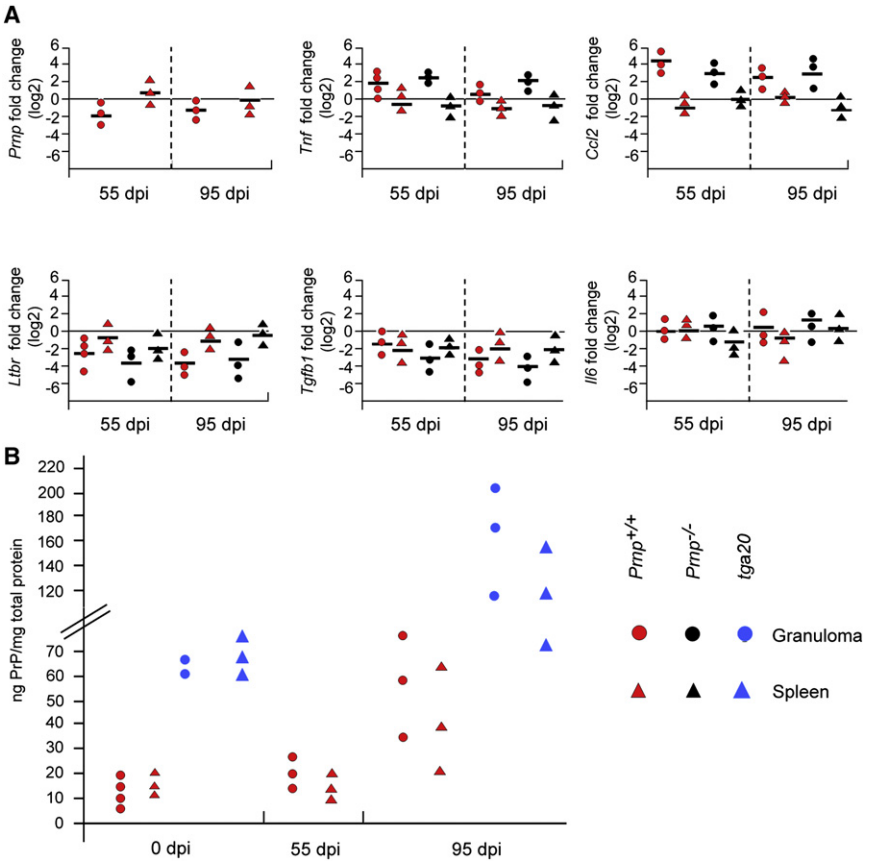

Figure 2. Molecular Characterization of Granulomas

(A) Real-time PCR analysis of *Prnp*, *Tnf*, *Ccl2*, *Ltβr*, *Tgfβ1*, and *Il6* mRNA expression in spleens (circles) and granulomas (triangles) of prion-inoculated $Prnp^{+/+}$ (red) and $Prnp^{-/-}$ (black) mice (55 and 95 dpi). Each data point represents the average of three measurements from one individual organ sample. The average of naive $Prnp^{+/+}$ spleens (n = 3) was set as the baseline. $Prnp^{-/-}$, $Ltβr^{-/-}$, and $Tnf^{-/-}$ mice were used as negative controls (n = 3, each; data not shown).

(B) PrP protein in spleens and granulomas of $Prnp^{+/+}$, $Prnp^{-/-}$, and *tga20* mice as detected by sandwich ELISA. Overall PrP levels increased over time ($Prnp^{+/+}$ spleens: p = 0.01; $Prnp^{+/+}$ granulomas: p = 0.04).

Molecular Characterization of Granulomas before and after Prion Inoculation

At 0, 55, and 95 dpi, *Prnp* mRNA expression in $Prnp^{+/+}$ granulomas was similar to or lower (50%–15%) than that of untreated or prion-inoculated $Prnp^{+/+}$ spleens (Figure 2A). In contrast, *Prnp* transcripts were not detectable in nongranulomatous $Prnp^{+/+}$ subcutaneous tissue or in $Prnp^{-/-}$ granulomas and spleens (data not shown).

Tnf and *Ccl2* transcripts in $Prnp^{+/+}$ and $Prnp^{-/-}$ granulomas at both 55 and 95 dpi were ~16- and 64-fold higher, respectively, than in $Prnp^{+/+}$ spleens and ≥128 fold higher than in nongranulomatous $Prnp^{+/+}$ subcutaneous tissue (Figure 2A). *Ltβr* mRNA expression in granulomas was ≤50%–10% less than in noninoculated $Prnp^{+/+}$ spleens (0, 55, and 95 dpi), whereas unaffected subcutaneous tissue contained very little *Ltβr* mRNA (Figure 2A). *Il6* and *Tgfβ1* were transcribed similarly in granulomas and spleens, yet were undetectable in unaffected subcutaneous tissue. The homeostatic chemokines *Ccl21*, *Cxcl13*, *Ccl19*, and *Cx3cl1* were weakly transcribed or undetectable in $Prnp^{+/+}$ and $Prnp^{-/-}$ granulomas and subcutaneous tissue (Figure S2). Hence, CFA-induced granulomas expressed relatively abundant *Prnp* transcripts and recapitulated the expression of proteins involved in the formation of human granulomas (Russell, 2007).

Quantification of PrP Protein in Granulomas

PrP^C concentrations in granuloma homogenates (CFA or Z/PFO induced) of $Prnp^{+/+}$ and *tga20* mice were similar to those of the respective spleens (Figure 2B and Figure S2B). Granulomas and spleens of *tga20* mice displayed 2- to 5-fold greater PrP concentrations than those of $Prnp^{+/+}$ mice. At 95 dpi, a rise in total PrP was observed in both granulomas and spleens, possibly reflecting deposition of PrP^{Sc}. No PrP^C protein was detected in normal $Prnp^{+/+}$ subcutaneous tissues and in spleens and granulomas of $Prnp^{-/-}$ mice (Figure 2B).

We then investigated *Prnp* promoter activity in granulomas of $Prnp^{GFP/GFP}$ mice whose PrP coding sequence was replaced by the green fluorescent protein (GFP) through gene targeting (Figure S3A). At 50 dpgi, GFP^+ cells were detected in centers, fibroblast cuffs, and fibrous capsules of $Prnp^{GFP/GFP}$ granulomas (Figure S3A). Two-channel fluorescence microscopy revealed *Prnp* promoter activity in many, but not all, $LTβR^+$ mostly stromal cells and some $I\text{-}A^+$, $I\text{-}E^+$, and $CD68^+$ macrophages (Figure S3B). Therefore, some stromal and hematopoietic cells within granulomas display *Prnp* promoter activity. Alternatively $CD68^+$ macrophages may have phagocytosed GFP^+ material.

PrP^{Sc} Is Produced Autochthonously within Granulomas

The presence of PrP^{Sc} at 55 and 95 dpi was assessed by sodium phosphotungstate (NaPTA) precipitation followed by immunoblot analysis of granuloma (Figure 3A, left panel) and spleen homogenates (Figure 3A, right panel). All $Prnp^{+/+}$ spleens displayed PrP^{Sc} at both 55 and 95 dpi (Figure 3A). $Prnp^{+/+}$ granulomas displayed PrP^{Sc} in one of three mice at 55 dpi, and in three of three mice at 95 dpi (Figure 3A and Figure S4A), whereas all $Prnp^{-/-}$ granulomas and spleens (n = 12) lacked PrP^{Sc} (Figure 3A and Figure S4A). We additionally tested whether spleens, granulomas, and skin (including superficial subcutaneous tissue) surrounding granulomas contained prion infectivity. Tissue homogenates derived from $Prnp^{+/+}$ and $Prnp^{-/-}$ mice (55 and 95 dpi) were injected intracerebrally (i.c.) into *tga20* indicator mice and monitored clinically (Figures 3B and 3C). $Prnp^{+/+}$ spleen homogenates displayed sizeable prion infectivity (4.3–5.5 $logLD_{50}$/g tissue) at 55 and

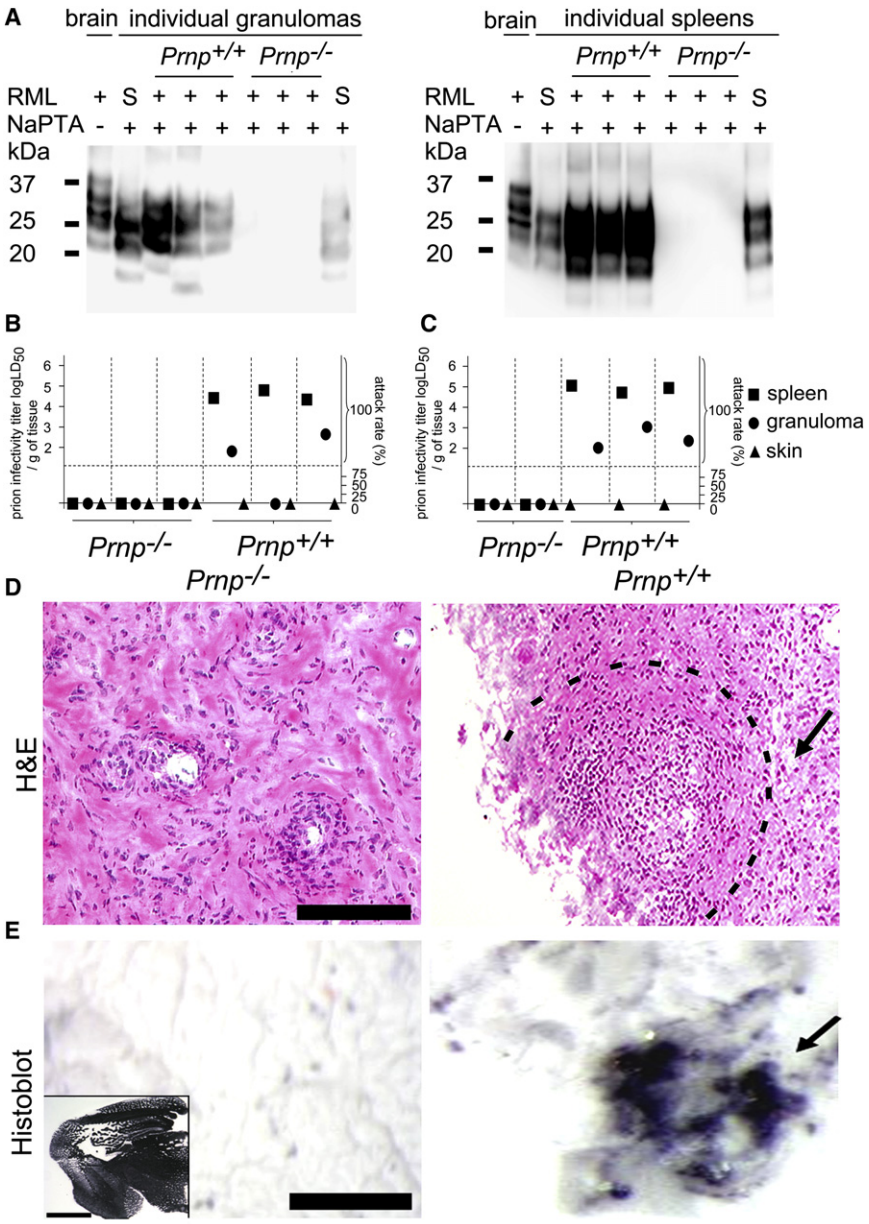

Figure 3. Prion Infectivity and PrP^{Sc} in Granulomas

(A) PrP^{Sc} detection by NaPTA-enhanced immunoblotting of granuloma (left panel) and splenic (right panel) homogenates from $Prnp^{+/+}$ and $Prnp^{-/-}$ mice (95 dpi). Scrapie-sick $Prnp^{+/+}$ brain homogenate (2.5 μg, first lane) and noninfected $Prnp^{-/-}$ granulomas (250 μl of a 10% w/v homogenate) spiked with scrapie-sick $Prnp^{+/+}$ brain homogenate (25 μg, lanes 2 and 9) were used as positive controls. "S" refers to spike. All homogenates except lane 1 were digested with proteinase K.

(B and C) Prion-infectivity titers of $Prnp^{+/+}$ and $Prnp^{-/-}$ spleen, granuloma, and skin homogenates isolated at (B) 55 and (C) 95 dpi. Infectivity titers were assessed by mouse bioassay. Vertical dotted lines separate individual $Prnp^{+/+}$ and $Prnp^{-/-}$ mice. Each symbol represents the average of three to four intracerebrally inoculated *tga20* mice. Values above the dashed horizontal line represent attack rates of 100%, whereas values below the line indicate that <100% of indicator animals developed scrapie.

(D and E) H&E staining (D) and corresponding histoblot analysis (E) of consecutive cryosections derived from granulomas of $Prnp^{-/-}$ and $Prnp^{+/+}$ mice at 95 dpi. PrP^{Sc} is located mainly within the fibroblast cuffs of granuloma nodules (indicated by arrows and dotted lines). Scale bars represent 150 μm. The inset in (E) shows a RML-inoculated scrapie-sick $Prnp^{+/+}$ brain, used as positive control. The scale bar represents 500 μm. No signal was detected in brains of RML-inoculated $Prnp^{-/-}$ mice.

95 dpi, whereas $Prnp^{+/+}$ granulomas had 1.8–2.6 $logLD_{50}$/g in two of three mice at 55 dpi and 1.9-3 $logLD_{50}$/g in three of three mice at 95 dpi (Figures 3B and 3C). $Prnp^{-/-}$ granuloma or skin homogenates derived from $Prnp^{+/+}$ and $Prnp^{-/-}$ mice lacked prion infectivity at 55 and 95 dpi. Each case of clinically diagnosed terminal prion disease was confirmed by histology and immunohistochemistry (Figure S4B).

To visualize PrP^{Sc} within granulomas, we performed histoblot analyses of granulomas from prion-inoculated $Prnp^{+/+}$ and $Prnp^{-/-}$ mice on consecutive cryosections (Figure 3D). PrP^{Sc} was found mainly within granuloma centers and fibroblast cuffs of $Prnp^{+/+}$ mice at 55 (data not shown) and 95 dpi (Figure 3E). Granulomas of prion-inoculated $Prnp^{-/-}$ mice were devoid of PrP^{Sc} (Figure 3E). Brain sections of RML-inoculated $Prnp^{+/+}$ and $Prnp^{-/-}$ mice were used for control (Figure 3E, insert). We conclude that both prion infectivity and PrP^{Sc} accumulate in granulomas.

Establishment of Chimeric Granulomas

We then sought to define the cellular compartment supporting PrP^{C} protein expression and prion replication. We performed reciprocal bone marrow (BM) reconstitution experiments ($Prnp^{+/+} \rightarrow Prnp^{+/+}$; $Prnp^{+/+} \rightarrow Prnp^{-/-}$; $Prnp^{-/-} \rightarrow Prnp^{+/+}$; and $Prnp^{-/-} \rightarrow Prnp^{-/-}$) and assessed reconstitution efficiency by flow-cytometry analysis for cell-surface PrP^{C} using Cy5-labeled POM2 antibody (Polymenidou et al., 2005). Reconstitution of $Prnp^{-/-}$ mice with $Prnp^{+/+}$ BM restored cell-surface PrP^{C} expression on peripheral lymphocytes similarly to $Prnp^{+/+}$ mice (Figure 4A and Figure S5A). Conversely, $Prnp^{+/+}$ mice reconstituted with $Prnp^{-/-}$ BM showed almost complete absence of PrP^{C}-expressing cells from peripheral blood (Figure 4A). Next, we induced granulomas in $Prnp^{+/+} \rightarrow Prnp^{-/-}$ and $Prnp^{-/-} \rightarrow Prnp^{+/+}$ chimeras, as well as in $Prnp^{-/-}$ and $Prnp^{+/+}$ mice. Granulomas and spleens of $Prnp^{+/+}$ and $Prnp^{-/-} \rightarrow Prnp^{+/+}$ mice displayed PrP^{C} concentrations of ca. 5–15 ng/mg tissue, whereas granulomas and spleens of $Prnp^{-/-}$ and $Prnp^{+/+} \rightarrow Prnp^{-/-}$ mice contained very little or <2 ng/mg PrP^{C} (Figure 4B, left panel). Therefore, PrP^{C} was

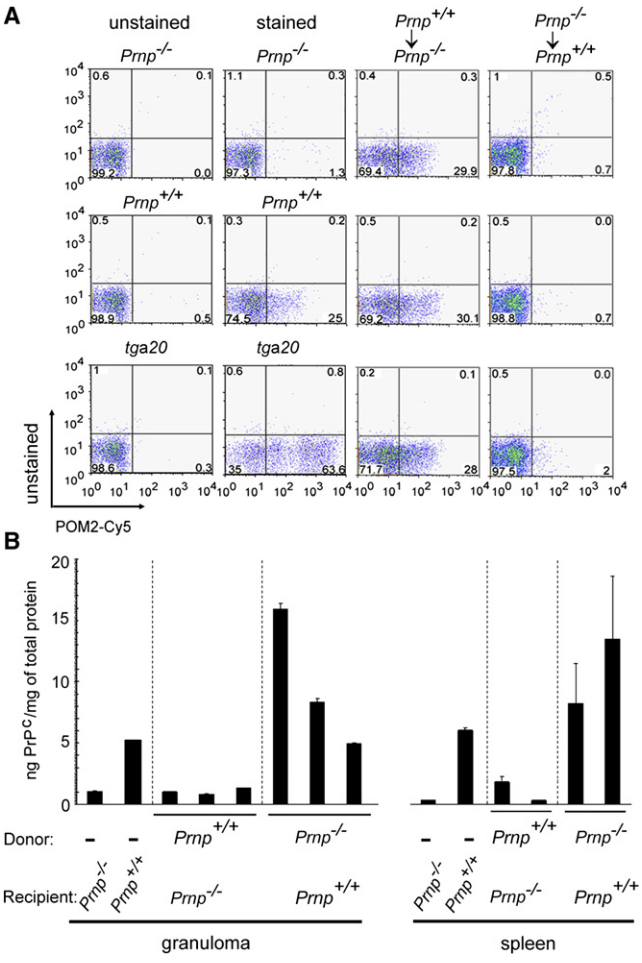

Figure 4. The Stromal Compartment of Granulomas Facilitates Efficient PrP^C Expression

(A) Flow-cytometry analysis of surface PrP^C expression in live-gated peripheral blood lymphocytes. Left two columns show unstained and POM2-Cy5 stained lymphocytes from peripheral blood of *Prnp*$^{-/-}$, *Prnp*$^{+/+}$, and *tga20* mice. Numbers in the quadrants represent the relative percentages of cells. Each panel represents one individual mouse.

(B) PrP^C content of granulomas and spleens as determined by ELISA at 50 dpgi. Each bar represents one individual mouse. Error bars indicate the standard deviation (SD) of three technical replicates.

predominantly produced by radioresistant cells in both granulomas and spleens.

Theoretically, PrP^C expression in granulomas of BM-chimeric mice (*Prnp*$^{-/-}$→*Prnp*$^{+/+}$) may be contributed by residual radioresistant hematopoietic cells. We addressed this by generating reciprocal β-Actin-GFP and C57BL/6 BM-chimeras (β-actin-GFP→C57BL/6 and C57BL/6→β-actin-GFP; Figures S5B and S5C). Reconstitution efficiency, as assessed by identification of donor-derived blood cells in C57BL/6 mice receiving β-actin-GFP BM, was 88%–94%. We then counted CD68$^+$GFP$^+$ and B220$^+$GFP$^+$ cells at 13 weeks after reconstitution (ca. 50 dpgi) in several serial sections of granulomas. In granulomas from three individual C57BL/6→β-Actin-GFP chimeric mice ca. 6% ± 3% of CD68$^+$ and 9% ± 4% of B220$^+$ cells were GFP$^+$. In contrast, in granulomas of β-actin-GFP→C57BL/6 chimeric mice (n = 3), the majority of CD68$^+$ (84% ± 4%) and B220$^+$ (83% ± 7%) cells were GFP$^+$ (Figures S5B and S5C). Therefore, very few if any residual B220$^+$ or CD68$^+$ radioresistant hematopoietic cells are present in granulomas and are unlikely to account for the relatively high PrP^C expression in granulomas of chimeric *Prnp*$^{-/-}$→*Prnp*$^{+/+}$ mice.

The Stromal Compartment of Granulomas Replicates Prions

We then investigated the contribution of the radioresistant compartment to prion pathogenesis within granulomas. Chimeric mice (*Prnp*$^{+/+}$→*Prnp*$^{-/-}$; *Prnp*$^{+/+}$→*Prnp*$^{+/+}$; *Prnp*$^{-/-}$→*Prnp*$^{-/-}$; and *Prnp*$^{-/-}$→*Prnp*$^{+/+}$) were inoculated i.p. with 5 logLD_{50} prions (RML6) at 50 dpgi, and analyzed at 95 dpi (Figures S6A and S6B). PrP^{Sc} in granulomas was assessed by NaPTA precipitation and then by immunoblot analysis. At 95 dpi, all *Prnp*$^{-/-}$→*Prnp*$^{+/+}$ and *Prnp*$^{+/+}$→*Prnp*$^{+/+}$ granulomas, but no *Prnp*$^{+/+}$→*Prnp*$^{-/-}$ and *Prnp*$^{-/-}$→*Prnp*$^{-/-}$ granulomas, displayed PrP^{Sc} (n = 6 in each group; Figures S6 and S7A).

To evaluate prion-infectivity titers, we performed scrapie cell assays (Klohn et al., 2003) in endpoint format (SCEPA) with spleen and granuloma homogenates from the same individual chimeric mice that had been subjected to immunoblot analysis. Brain homogenates derived from terminally scrapie-sick or healthy mice were used for calibrating and ascertaining the detection limit of the SCEPA (Supplemental Data). Sustained prion infectivity was detected in all *Prnp*$^{+/+}$→*Prnp*$^{-/-}$ (n = 4), *Prnp*$^{+/+}$→*Prnp*$^{+/+}$ (n = 2), and *Prnp*$^{-/-}$→*Prnp*$^{+/+}$ spleens (n = 4), but not in *Prnp*$^{-/-}$→*Prnp*$^{-/-}$ spleens (n = 2) (Figure 5A, Figures S6 and S8, and Table 1), in agreement with previous reports (Blättler et al., 1997; Kaeser et al., 2001; Priller et al., 2006).

Chimeric *Prnp*$^{+/+}$→*Prnp*$^{+/+}$ and *Prnp*$^{-/-}$→*Prnp*$^{+/+}$ granulomas (n = 7) displayed titers of ≥6.1 log TCI units/g (Figure 5B, Figure S8, and Table 1), whereas no infectivity was detectable in *Prnp*$^{+/+}$→*Prnp*$^{-/-}$ and *Prnp*$^{-/-}$→*Prnp*$^{-/-}$ granulomas (n = 6). Therefore, prion-infectivity titers in granulomas of *Prnp*$^{-/-}$ BM recipients were consistently ≥3.3 logs lower than those of *Prnp*$^{+/+}$ recipients (Table 1).

Administration of soluble dimeric LTβR leads to the rapid disappearance of FDCs from spleen (Mackay and Browning, 1998) and was previously found to interfere with splenic prion replication (Aguzzi and Heikenwalder, 2006; Mabbott et al., 2000; Montrasio et al., 2000). Because granulomas expressed LTβR (Figure 2), prion replication within granulomas may also depend on LT signaling. We examined this question by treating granuloma-bearing, prion-infected mice with LTβR-Fc. Fifty dpgi, we inoculated mice i.p. with prions (RML5; 5 logLD_{50}). At 55 dpi, we injected either LTβR-Fc or pooled human immunoglobulins (Hu-IgG) as control (100 μg/injection) (Montrasio et al., 2000) weekly for up to 6 weeks. Neither LTβR-Fc nor Hu-IgG treatment was found to exert any effect on the size of granulomas (data not shown). Immunohistochemistry and histoblot analyses confirmed the dedifferentiation of FDCs and suppression of splenic PrP^{Sc} accumulation in LTβR-Fc treated, but not in Hu-IgG treated, mice (Figures S7B and S7C).

Granulomas were then isolated and homogenized, and prion-infectivity titers were determined by SCEPA (Klohn et al., 2003) (Figure 5C, Figure S8, and Table 1). All Hu-IgG treated granulomas displayed prion-infectivity titers of ≥4 log TCI units/g. In

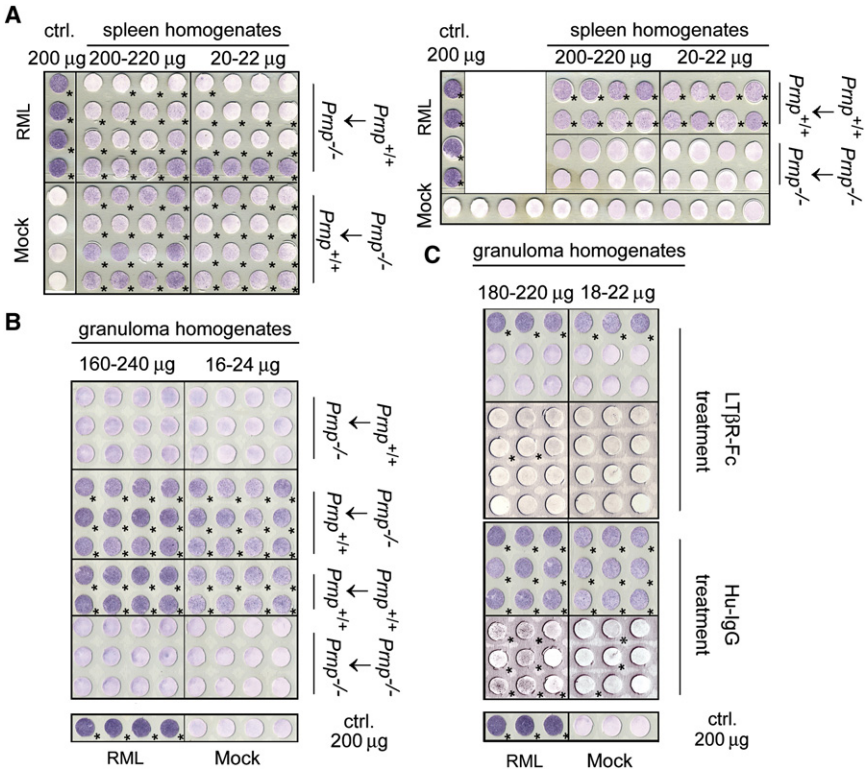

Figure 5. Prions Accumulate in a Radioresistant, LTβR-Signaling-Dependent Compartment of Granulomas

Prion-infectivity titers of spleens and granulomas were determined by scrapie cell assay in endpoint format (SCEPA). Transfer of prion infectivity to cells results in PrP^{Sc+} colonies, which in turn confer a spotted dark stain to ELISPOT membranes. Membranes with >3 PrP^{Sc+} colonies (asterisks) were regarded as infected.

(A) Prion infectivity in splenic homogenates of chimeric $Prnp^{+/+} \rightarrow Prnp^{-/-}$, $Prnp^{-/-} \rightarrow Prnp^{+/+}$ (left panel), and $Prnp^{+/+} \rightarrow Prnp^{+/+}$ mice but not in spleens of $Prnp^{-/-} \rightarrow Prnp^{-/-}$ mice (right panel; see also Table 1). Positive (RML6; 300,000 LD_{50} units in 200 µg) and negative (Mock: healthy mouse brain homogenate; 200 µg) controls are indicated. Each row represents an individual mouse. The range of granuloma-derived protein added per well is indicated.

(B) Prion infectivity in chimeric granulomas with a $Prnp^{+/+}$ stromal compartment ($Prnp^{+/+} \rightarrow Prnp^{+/+}$ and $Prnp^{-/-} \rightarrow Prnp^{+/+}$ mice). "Ctrl." refers to controls. Each row represents an individual mouse.

(C) Effect of LTβR-Fc or Hu-IgG treatment on prion infectivity of granulomas. Whereas Hu-IgG treatment had no effect on prion content of granulomas (n = 6), LTβR-Fc treatment suppressed prion titers in five of seven granulomas. Each row represents an individual mouse. Horizontal lines demarcate two independent experiments. "Ctrl." refers to controls.

contrast, no infectivity was detected in five of seven granulomas treated with LTβR-Fc fusion protein (detection threshold: 2.8 log TCI units/g). The two remaining granulomas displayed 3.5 and ≥4.8 log TCI units/g (Figure 5C and Table 1). Therefore, LTβR-Fc treatment markedly reduced the prion load of granulomas ($p < 0.02$).

Identity of Prion-Replicating Cells in Granulomas

We first compared the number and size distribution of dissociated cells from untreated, LTβR-Fc, or Hu-IgG treated granulomas as well as from naive spleens by flow cytometry (Figure 6A and Figures S9 and S10). The morphological identity of recovered cells was confirmed by Papanicolaou-stained cytospin preparations. Whereas splenic cell suspensions contained lymphocytes (6–7 µm) and larger cells (macrophages and granulocytes, 8–9 µm), granulomas were almost exclusively composed of larger cells (macrophages, granulocytes, and fibroblasts, etc.; Figure 6A and Figure S9). The viability of granulomas treated with LTβR-Fc or Hu-IgG was 65% ± 18% and 66% ± 7%, respectively ($p = 0.9$).

Flow-cytometry analysis revealed a mostly $CD45^-$, GFP^+ cell population within granulomas of $Prnp^{GFP/GFP}$ mice (Figure 6A).

Table 1. Quantitative Prion-Infectivity Determinations in Granulomas, Spleens, and Brains

Mouse	Organ	Treatment	dpi	Log TCI Units/g of Tissue
CD1	brain (RML6 standard)	-	pooled	8.3, 8.3 (two independent determinations)
$Prnp^{-/-} \rightarrow Prnp^{+/+}$	spleen	-	95	≥6.1 in 4/4 mice
$Prnp^{+/+} \rightarrow Prnp^{-/-}$	spleen	-	95	≥6.1 in 4/4 mice
$Prnp^{+/+} \rightarrow Prnp^{+/+}$	spleen	-	95	≥6.1 in 2/2 mice
$Prnp^{-/-} \rightarrow Prnp^{-/-}$	spleen	-	95	≤ 2.8 in 2/2 mice
$Prnp^{-/-} \rightarrow Prnp^{+/+}$	granuloma	-	95	≥6.1 in 3/3 mice
$Prnp^{+/+} \rightarrow Prnp^{-/-}$	granuloma	-	95	≤2.8 in 3/3 mice
$Prnp^{+/+} \rightarrow Prnp^{+/+}$	granuloma	-	95	≥6.1 in 3/3 mice
$Prnp^{-/-} \rightarrow Prnp^{-/-}$	granuloma	-	95	≤2.8 in 3/3 mice
$Prnp^{+/+}$	granuloma	LTβR-Fc	95	≥4.8 in 1/7 mice, =3.5 in 1/7 mice, ≤2.8 in 5/7 mice
$Prnp^{+/+}$	granuloma	Hu-IgG	95	≥4.8 in 4/6 mice, =4 in 2/6 mice

Titers were calculated as described (Klohn et al., 2003). Infectivity was assessed by SCEPA.

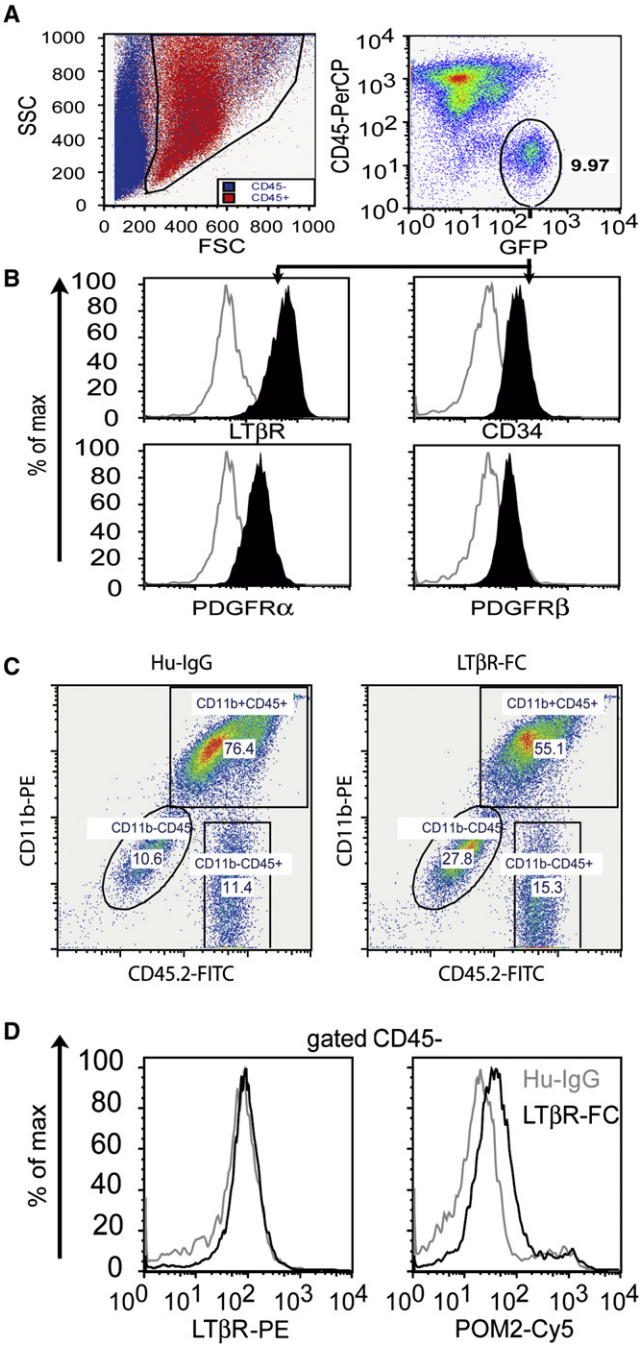

Figure 6. LTβR-Fc Treatment Does Not Change PrP^C Expression on Stromal Cells of Granulomas

(A) Flow-cytometry analysis of granulomas derived from *Prnp*$^{GFP/GFP}$ and wild-type mice treated with Hu-IgG or LTbR-Fc. The upper-left panel shows forward (FSC) and sideward scatter (SSC) and live gate (black gate) of a granuloma cell suspension. The upper-right panel shows a dot plot depicting the GFP$^+$CD45$^-$ population detected in unstained granuloma cell suspensions of *Prnp*$^{GFP/GFP}$ mice (9.97% of all granuloma cells). Fluorescent intensities are depicted in a log scale.

(B) Histograms characterizing the gated GFP$^+$ cell population of *Prnp*$^{GFP/GFP}$ granuloma for the expression of various markers. GFP$^+$CD45$^-$ cells were LTbR$^+$, CD34$^+$, and PDGFRab$^+$ (black graphs). Hollow, gray graphs depict the appropriate isotype controls used.

(C) Flow-cytometry analysis of Hu-IgG or LTbR-Fc treated, live-gated wild-type granuloma cell suspensions for CD11b$^+$CD45$^+$, CD45$^-$PrP$^+$ (left panel) or CD45$^-$LTbR$^+$ (right panel) granuloma cell populations.

(D) Flow-cytometry analysis of Hu-IgG or LTbR-Fc treated, live-gated, CD45$^-$ wild-type granuloma cell suspensions for PrP^C or LTbR surface expression. LTbR-Fc- (black graph) or Hu-IgG- (hollow, gray graph) treated mice are indicated. Mean fluorescence intensities (MFIs) for PrP^C surface expression are as follows: LTbR-Fc: 140 ± 12; Hu-IgG: 133 ± 12; p = 0.5; MFI for LTbR surface expression: LTbR-Fc: 204 ± 34; Hu-IgG: 209 ± 5; p = 0.8). At least three independent experiments were performed.

Although the great majority of CD45$^-$ granuloma cells expressed podoplanin (gp38), CD45$^-$GFP$^+$ cells were gp38$^-$ and did not appear to express vascular cell adhesion molecule-1 (VCAM-1) or platelet and endothelial cell adhesion molecule-1 (CD31 or PECAM) (Figure S10). Further characterization of the CD45$^-$GFP$^+$ population revealed that those cells express LTβR and CD34 and are positive for platelet-derived growth factor receptors α and β (PDGFRα and β), suggesting a mesenchymal origin (Figure 6A and Figure S10). This was also reproduced in granulomas of wild-type mice, in which we could identify the same CD45$^-$PrP$^+$LTβR$^+$ population (Figure S10).

Six weeks of LTβR-Fc or Hu-IgG treatment did not significantly affect the main cell populations within granulomas. Flow-cytometry analysis identified a slight reduction of CD11b$^+$CD45$^+$ macrophages in LTβR-Fc treated granulomas (LTβR-Fc: 56 ± 5; Hu-IgG: 72 ± 10; p = 0.06; Figure 6B), and the number of CD45$^-$PrP$^+$LTβR$^+$ cells was unchanged (LTβR-Fc: 5.6% ± 3%; Hu-IgG: 5.1% ± 3%; p = 0.88) (Figure 6C). Immunostains (CD11b, CD11c, MHCII, FDC-M1, CD3, and B220) failed to reveal differences between LTβR-Fc- and Hu-IgG-treated granulomas (Figure S11). *Prnp* and *Ltβr* transcription and PrP^C protein concentration were similar in LTβR-Fc- and Hu-IgG-treated granulomas (Figure S12). However, LTβR-Fc-treated granulomas displayed significantly reduced mRNA expression of the LTβR targets *Ccl2* (25%–5% ; p < 0.05) and *Icam1(50%–5%,* p < 0.05), but not of *Ccl5* and *Vcam1*.

DISCUSSION

Chronic inflammatory conditions are ubiquitous in the entire animal kingdom, ranging from autoimmunity to bacterial, fungal, and viral infections and persistent foreign bodies. Each of these pathogenetic groups is associated with distinct morphological and cellular features. Autoimmune diseases and chronic bacterial infections can induce lymphoid follicles with prominent FDC networks (Drayton et al., 2006), which can replicate prions in mice (Heikenwalder et al., 2005; Seeger et al., 2005), sheep (Ligios et al., 2005), and deer (Hamir et al., 2006). However, chronic inflammation more commonly gives rise to granulomas (Kumar et al., 2004) whose cellular composition is different from that of lymphoid follicles. Granulomas occur, for example, in Crohn's disease, sarcoidosis (Iannuzzi et al., 2007), and most mycobacterial (Britton and Lockwood, 2004; Ernst et al., 2007; Russell, 2007), fungal, and parasitic infections, as well as in foreign-body reactions. Because of their importance for human and veterinary medicine, we sought to determine whether granulomas may have prion-replication competence.

We found that granulomas displayed surprisingly high PrP^C concentrations approaching the relatively high levels seen in

spleens. Because healthy subcutaneous tissue did not express detectable PrP^C mRNA or protein, some granuloma-specific cells must thus express very high amounts of PrP^C. This finding applied to both CFA and Z/PFO-induced granulomas despite their markedly different cellular composition.

Reciprocal bone-marrow grafting experiments indicated that radioresistant cells accounted for most of the PrP^C found in granulomas, whereas radiosensitive cells did not appreciably contribute to the PrP^C content of granulomas. Hence, granulomatous inflammation induces PrP^C expression in preexisting stromal cells or maybe leads to the mobilization and recruitment of PrP^C-expressing stromal cells originally residing at other sites.

Granulomas of prion-inoculated *Prnp*$^{+/+}$ mice were found to consistently display PrP^{Sc} and prion infectivity. This was surprising because granulomas lacked FDCs, which are essential to lymphoid and extraneural prion replication in several paradigms (Hamir et al., 2006; Heikenwalder et al., 2005; Ligios et al., 2005; Mabbott et al., 2000; Montrasio et al., 2000).

Granulomas lacked *Mfge8* mRNA, an early marker of FDC differentiation (Kranich et al., 2008). We therefore investigated whether the above results may stem from inoculum retention rather than local prion replication. This, however, is unlikely because (1) granulomas of *Prnp*$^{-/-}$ mice were always devoid of infectivity and (2) the proportion of prion-positive granulomas at 95 dpi was greater than at 55 dpi, whereas simple prion retention would intuitively be expected to decrease over time. Alternatively, infectivity of granulomas may plausibly represent "spill-over" from other extraneural sites of prion replication, such as the lymphoid organs. However, granulomas of *Prnp*$^{+/+}$ → *Prnp*$^{-/-}$ chimeric mice completely lacked any prion infectivity, although their spleens displayed prion-infectivity titers similar to those of wild-type mice (Blättler et al., 1997; Kaeser et al., 2001; Priller et al., 2006). This finding suggests that prion uptake from other sites of replication is highly unlikely. Notably, homogenates of skin located in the immediate vicinity of granulomas lacked prion infectivity in both *Prnp*$^{+/+}$ and *Prnp*$^{-/-}$ mice at 55 and 95 dpi. This is in agreement with the report that the skin may carry prions only at late stages of disease (Thomzig et al., 2007).

Our findings unambiguously indicate that prions replicate in the nonhematopoietic compartment of granulomas. The latter contains predominantly fibroblasts, which were found to replicate prions in vitro (Vorberg et al., 2004), and—to a much lesser extent—endothelia, pericytes, and possibly some nerve endings and contaminating skin constituents. Some of these cell types (notably including fibroblasts) cannot be unequivocally identified with unique markers, and current technology does not allow for identifying prion replication at the single-cell level. Therefore, we opted to define the nature of the cells enabling granulomatous prion replication by virtue of their dependence on specific signaling pathways.

Prion invasion of spleen, lymph nodes, and Peyer's patches is completely dependent on lymphotoxin signaling (Mabbott et al., 2000; Montrasio et al., 2000). Because the latter is required for the differentiation and maintenance of FDCs (Mackay and Browning, 1998; Mackay et al., 1997), it was initially speculated that FDCs may be obligatorily required for extraneural prion replication. However, a growing body of evidence suggests a more nuanced situation. Although crucially dependent on lymphotoxin signaling in all conditions investigated, extraneuronal prion replication was found to occur in the absence of immunohistochemically recognizable FDCs in various paradigms (Dlakic et al., 2007; Kovacs et al., 2004; Oldstone et al., 2002; Prinz et al., 2002; Vorberg et al., 1999). Accordingly, *Tnfr1*$^{-/-}$ mice accumulate prions in lymph nodes despite the absence of FDCs, whereas mice deficient in LTs or their receptor are largely resistant (Klein et al., 1997; Prinz et al., 2002).

Although they did not contain any FDCs, granulomas expressed almost equal amounts of *Ltβr* mRNA as *Prnp*$^{+/+}$ spleens. LTβR-Fc treatment did not alter PrP^C expression but suppressed prion replication within granulomas by at least two orders of magnitude without affecting their formation, maintenance, and overall morphology. These results indicate that stromal cells other than FDCs can acquire prion-replication competence in vivo in a LTβR-signaling-dependent manner. What is the nature of these cells? A plausible candidate is the fibroblastic reticular cell (FRC) that was identified within lymphoid organs (Link et al., 2007) and possibly at inflammatory lesions (G. Eberl et al., personal communication). FRC maintenance and function depend on LTβR signaling (Scandella et al., 2008). All these characteristics are congruent with the defining traits of prion-replicating cells within granulomas. FRC maturation relies on interactions with LT-expressing lymphoid tissue inducer cells (LTis), suggesting that LTis may play a major role in prion pathogenesis.

We characterized the PrP^C-expressing stromal cell within granulomas in more detail by flow-cytometry analysis and additionally investigated the effects of LTβR-Fc treatment on granulomas. The prion-replicating cells within granulomas display overlapping features with FRCs of secondary lymphoid organs, given that FRCs also express LTβR (Link et al., 2007) and PrP^C (S. Luther, personal communication). However, prion-replicating cells within granulomas are most likely mesenchymal because they express PDGFRα and β and are not classical $CD45^-gp38^+VCAM\text{-}1^+$ FRCs (Link et al., 2007) because granulomas lacked *Ccl19* and *Ccl21*. It is possible that those cells stem from FRC progenitors undergoing atypical differentiation.

LTβR-Fc treatment did not deplete $CD45^-gp38^-CD31^-VCAM\text{-}1^-CD34^+PDGFR\alpha\beta^+$ $PrP^+LT\beta R^+$ cells nor did it markedly reduce the expression of PrP^C or LTβR, yet it reduced expression of a number of LTβR target genes. Therefore, LT signaling is likely to play an important role in licensing prion replication to granulomas independently of the formation of lymphoid follicles, the maturation of FDCs, and the expression of Mfge8. Because granulomas can occur at any site of the body, these results suggest that prions may colonize a broader spectrum of organs than previously anticipated. With respect to the relevance of the above findings for hospital hygiene (e.g., iatrogenic prion transmission in humans) and for veterinary medicine (e.g., prion shedding in animals), it will be interesting to test whether prion replication in granulomas occurs in farm animals and in humans.

EXPERIMENTAL PROCEDURES

Mice and Scrapie Inoculation

C57BL/6, congenic C57BL/6 β-actin-GFP mice (Jackson Laboratories) (Okabe et al., 1997), C57BL/6 × 129Sv (*Prnp*$^{+/+}$), *Prnp*$^{-/-}$ (Büeler et al., 1992), *Ltβr*$^{-/-}$, *Ltα*$^{-/-}$, *Mfge8*$^{-/-}$ (De Togni et al., 1994; Futterer et al., 1998;

Hanayama et al., 2004), and *tga20* (Fischer et al., 1996) mice were maintained under specific pathogen-free (SPF) conditions. Housing and experimental protocols were in accordance with the Swiss Animal Protection Law and in compliance with the regulations of the Veterinäramt, Kanton Zürich. Mice were infected intraperitoneally (i.p.) with 100 μl brain homogenate derived from terminally scrapie sick CD-1 mice. Brain material was homogenized in PBS/0.32M sucrose, containing 5 $\log LD_{50}$ of the Rocky Mountain laboratory (RML) scrapie strain (passage 5) (Kaeser et al., 2001) or RML6 (Falsig et al., 2008). Mice were euthanized at 0, 55, and 95 dpi in accordance with the standard operating procedures and the Swiss Animal Protection Law.

Generation of Chimeric Mice

A total of 1 to 2 × 10^7 BM cells were isolated from tibiae and femurs and injected into tail veins of 8- to 12-week-old recipients conditioned by whole-body irradiation (1100 rad). Six to eight weeks after grafting, reconstitution was assessed by FACS analysis of peripheral blood taken from the tail vein.

Induction of Granulomas

Granulomas were induced subcutaneously (s.c.) at two symmetric abdominal sites (left and right) in C57BL/6, β-*actin-GFP*, C57BL/6 × 129Sv (wild-type), $Prnp^{GFP/GFP}$, *tga20*, and $Prnp^{-/-}$ mice by CFA or Z/PFO emulsified in the identical amount of sterile PBS. At 25 dpgi, a second injection was performed in the immediate vicinity of the injection site. For analysis, granulomas were dissected, pooled, and subjected to immunohistochemical and WB analysis, ELISA, RNA purification, transmission assay and SCEPA.

LTβR-Fc and Hu-IgG Treatment

$Prnp^{+/+}$ mice were i.p. injected weekly with 100 μg LTβR-Fc or Hu-IgG (kindly provided by J. Browning; Biogen). Treatment was performed for 6 weeks.

Statistical Analysis

The effect of LTβR-Fc and Hu-IgG treatment on prion replication in granulomas of mice was analyzed with ordinal variables with three categories (<2.8, 2.8–4.8, and > 4.8 log TCI units). SPSS 15.0 (SPSS, Inc.) was used for statistical analyses. Groups were compared with the Mann-Whitney test with exact p values. For other statistical analyses, Student's t tests were performed.

Histology, Histoblot, and Immunohistochemistry

Paraffin sections (2 μm) and frozen sections (5 or 10 μm) of spleen, granuloma, and brain were stained with hematoxylin and eosin or various primary and secondary antibodies (Supplemental Data). Histoblot analysis was performed as described (Taraboulos et al., 1992).

RNA Isolation from Granulomas and Real-Time PCR Analysis

Flash-frozen granulomas were dissolved in RNA isolation buffer (RLT; QIAGEN) and homogenized with a homogenizer (Dispomix, Medic Tools). RNA was purified as described by the manufacturer's manual (QIAGEN). cDNA generation was performed with a QuantiTect, Reverse Transcription kit (Cat. No. 205313), and real-time PCR analysis was performed as recently described with a QuantiFast SYBR Green PCR kit (Cat. No.204052) (Heikenwalder et al., 2005). Primer combinations used are indicated in the Supplemental Data.

PrP Sandwich ELISA

Ninety-six-well plates were coated with 400 ng/ml of purified POM1 antibody overnight at 4°C. Plates were washed with PBS containing 0.1% (vol/vol) Tween 20 (PBST) and blocked with 5% Top Block for 2 hr at room temperature (RT). After washing, plates were incubated with 100 μl of granuloma homogenates containing 1 mg/ml total protein. Protein content of granuloma homogenates was assessed by a standard colorimetric method based on bicinchoninic acid (BCA, Pierce). Samples were analyzed in quadruplicates. For the standard curve, 2-fold serial dilutions of recombinant mouse $PrP_{23\text{-}230}$ in PBST/1% Top Block were applied (volume 100 μl), starting from a 50 ng/ml concentration. After 1 hr at RT, plates were washed extensively and then probed with biotinylated POM2 (Polymenidou et al., 2005) at a concentration of 200 ng/ml in PBST containing 1% Top Block for 1 hr at room temperature. After washing, plates were incubated with horseradish peroxidase-conjugated Avidin (1:5000 dilution, Invitrogen) for 1 hr at RT. Plates were developed with 2.2-azino-diethyl-benzothiazolinsulfonate (Boehringer), and optical density was measured at 405 nm. With the limiting dilution of recombinant mouse $PrP_{23\text{-}230}$ solutions of known concentrations, a standard curve was generated. On the basis of the standard curve, we calculated PrP^C concentration in each well containing sample. Standard deviation was calculated from technical quadruplicates of the samples. Limit of detection is ~2 ng/ml, representing 2× background level. In rare cases, we observed that $Prnp^{-/-}$ granuloma samples displayed increased background levels (up to 4 ng/ml). In those cases, averaged background values were subtracted from $Prnp^{+/+}$ values.

Flow-Cytometric Analysis

Prior to FACS analysis, each granuloma was isolated, and caseous liquid was removed and enzymatically digested in 4 ml RPMI containing 10% FCS, 3 mg/ml Collagenase D (Roche), and 0.8mg/ml DNase (Sigma) for 1 hr at 37°C. Released cells were filtered through a 70 μm nylon mesh, collected by centrifugation, resuspended in PBS containing 2% FCS, and filtered again through a 40 μm nylon mesh. The cells were then incubated with various primary and secondary antibodies (Supplemental Data).

Generation of $Prnp^{GFP/GFP}$ Mice

The two step "tag-and-exchange" method of gene-targeting was used to replace the entire protein coding sequence of the PrP gene (*Prnp*) with DNA sequence encoding the enhanced green fluorescent protein (EGFP) in mouse embryonic stem cells (ESCs) (Moore et al., 1995; Selfridge et al., 1992) (Figure S3A). For the first step, a "tag construct" undergoes homologous recombination with one endogenous *Prnp* allele, resulting in deletion of a section of *Prnp* and insertion of a hypoxanthine phosporibosyltransferase (Hprt) minigene, resulting in a knockout allele. The presence of the *Hprt* minigene confers resistance to HAT media, which will kill ESCs not integrating the *Hprt* minigene. For the second step, knockout ESCs were modified with an exchange construct replacing the *Hprt* minigene with the EGFP sequence by homologous recombination. The *Prnp*-GFP allele differs from the wild-type *Prnp* allele by the inclusion of a BamHI restriction endonuclease site adjacent to the EGFP coding sequence, detected by genomic Southern analysis with a probe homologous to a region of *Prnp* downstream of the targeting constructs. Correctly targeted ESCs were injected into 3.5 day P.C. embryos from C57BL/6 Taconic mice. Injected embryos were then implanted into pseudopregnant females (CD1). We then bred chimeric mice to C57Bl/6 mice to establish the $Prnp^{GFP/GFP}$ mouse line.

Scrapie Cell Assay in End Point Format

This assay was performed as previously described by (Klohn et al., 2003). Replicate aliquots of highly prion-susceptible neuroblastoma cells (subclone N2aPK1) were placed into 4–24 wells of a 96-well plate and exposed to inoculum control (RML6) or prion samples (granuloma and splenic tissue homogenized and diluted from 10^{-3} to 10^{-6}) for 3 days, split 1:3 three times every 2 days, and split 1:10 four times every 3 days. After reaching confluence, 2 × 10^4 cells from each well were filtered onto the membrane of an ELISPOT plate (Millipore; MultiScreenHTS filter plates with Immobilon-P PVDF membrane), treated with PK and denatured, and individual infected (PrP^{Sc}-positive) cells were detected immunochemically with PrP antibody POM1 to PrP (Polymenidou et al., 2005). Wells were scored positive if the spot number exceeded mean background values added by three times the standard deviation of the MOCK control. Here, an ELISPOT membrane with ≥3 PrP^{Sc+} colonies (asterisks) was regarded as infected (see Figure 5). From the proportion of negative to total wells, the number of tissue culture infectious units per ml was calculated with the Poisson equation.

In two independent experiments, a 10^{-8} dilution of a standard inoculum (brain homogenate from a terminally scrapie-sick mouse) yielded 11/24 or 12/24 positive wells, corresponding to a titer of ~8.3 log tissue culture infectivity (TCI) units/g of brain tissue for the initial inoculum (Figures S6 and S8 and Table 1). The sensitivity threshold was calculated to be 2.8 log TCI units/g of brain tissue.

Infectivity Bioassay with tga20 Indicator Mice

Assays were performed on 10% splenic, granuloma, and cutaneous homogenates. For granuloma homogenization, granulomas were isolated from the subcutis and skin and fatty tissue were removed. Granulomas were chopped

with two scalpel blades. Skin adjacent to granulomas was isolated and approximately 1–2 cm^2 were used for homogenization. All tissues were diluted in PBS, homogenized with a homogenizer (Precellys 24; Bertin Technologies) in four rounds of homogenization (depending on the tissue) for 30 s, and subsequently cooled on ice for 5 min between each cycle. When homogenous, solution was spun for 1 min at 500 g. Supernatants (30 μl) of granuloma, cutaneous, and splenic homogenates were inoculated intracerebrally into groups of three to four *tga20* mice (Fischer et al., 1996). *Tga20* mice were monitored until the terminal stage of disease and euthanized according to the standard operating procedures. The relationship $y = 11.45 - 0.088x$ (y, log LD_{50} per milliliter of homogenate; x, incubation time in days to terminal disease) was calculated by linear regression (Kaeser et al., 2001; Prusiner et al., 1982).

Immunoblot Analysis and Sodium Phosphotungstate Precipitation

Tissue homogenates (brain and spleen) were adjusted to 8 mg/ml protein and treated with proteinase K (20–50 μg/ml, 30 min, 37°C). We electrophoresed 50 μg total protein through a SDS-PAGE gel (12%). Proteins were transferred to nitrocellulose by wet-blotting. Membranes were blocked (TBST containing 5% nonfat milk), decorated with monoclonal antibody POM1 (Polymenidou et al., 2005), and visualized by enhanced chemiluminescence (ECL, Socochim, Pierce). For granuloma homogenates NaPTA precipitation was performed. 10% granuloma homogenates were prepared in PBS on ice. Gross cellular debris was removed by centrifugation at 500 g for 1–2 min. The resulting supernatant was adjusted to 500 μl with PBS and mixed 1:1 with 4% Sarkosyl in PBS. Samples were incubated for 15 min at 37°C under constant agitation. Benzonase and $MgCl_2$ were added to a final concentration of 50 U/ml and 1 mM, respectively, and incubated for 30 min at 37°C under agitation. Prewarmed NaPTA stock solution (pH 7.4) was added to a final concentration of 0.3%, and the sample was incubated at 37°C for 30 min with constant agitation and then centrifuged at 37°C for 30 min at 14000 g in an Eppendorf microcentrifuge. The pellet was resuspended in 30 μl 0.1% Sarkosyl in PBS and digested with 30 μg/ml proteinase K (PK) for 60 min at 37°C with agitation. The sample was heated at 95°C for 5 min in SDS-containing loading buffer before loading onto 12% Novex SDS polyacrylamide gels (Invitrogen).

SUPPLEMENTAL DATA

Supplemental Data include Supplemental Experimental Procedures and twelve figures and can be found with this article online at http://www.immunity.com/supplemental/S1074-7613(08)00512-8.

ACKNOWLEDGMENTS

We thank J. Browning for discussions and for kindly providing Hu-IgG and LTβR-Fc, B. Seifert for help with statistical analyses, C. Julius, P. Schwarz, M. Wagner, R. Moos, A. Marcel, B. Odermatt, A. Fitsche, S. Behnke, and M. König for technical support, B. Ludewig for kindly providing *plt*/*plt* mice, and S. Luther for critical reading and supplying anti-CD31, CD34, and PDGFRα/β antibodies. This work was supported by grants of the Bundesamt für Bildung und Wissenschaft, Neuroprion (Priogen) (A.A.), the Ernst-Jung-Foundation, the Stammbach foundation (A.A.), ImmunoPrion, FP6-Food-023144, 2006-2009 (A.A.), the Swiss National Science Foundation (A.A.), and the NCCR on neural plasticity and repair (A.A.). M.H. was supported by the Bonizzi-Theler foundation, the Swiss MS Society, the Prof. Dr. Max Cloëtta foundation, the Oncosuisee-foundation (02113-082007), and the Kurt and Senta Hermann foundation. M.H., M.M., and J.B. were supported by the Hartmann Müller foundation and a Career Award of the University of Zürich, respectively. This work was supported by funding from the United States Department of Defense (S.L.) and an NIH postdoctoral fellowship (W.S.J.).

Received: May 8, 2008
Revised: September 10, 2008
Accepted: October 13, 2008
Published online: December 18, 2008

REFERENCES

Aguzzi, A., and Heikenwalder, M. (2006). Pathogenesis of prion diseases: Current status and future outlook. Nat. Rev. Microbiol. *4*, 765–775.

Aguzzi, A., and Polymenidou, M. (2004). Mammalian prion biology. One century of evolving concepts. Cell *116*, 313–327.

Aguzzi, A., and Weissmann, C. (1997). Prion research: The next frontiers. Nature *389*, 795–798.

Andreoletti, O., Simon, S., Lacroux, C., Morel, N., Tabouret, G., Chabert, A., Lugan, S., Corbiere, F., Ferre, P., Foucras, G., et al. (2004). PrPSc accumulation in myocytes from sheep incubating natural scrapie. Nat. Med. *10*, 591–593.

Blättler, T., Brandner, S., Raeber, A.J., Klein, M.A., Voigtländer, T., Weissmann, C., and Aguzzi, A. (1997). PrP-expressing tissue required for transfer of scrapie infectivity from spleen to brain. Nature *389*, 69–73.

Brandner, S., Isenmann, S., Raeber, A., Fischer, M., Sailer, A., Kobayashi, Y., Marino, S., Weissmann, C., and Aguzzi, A. (1996). Normal host prion protein necessary for scrapie-induced neurotoxicity. Nature *379*, 339–343.

Britton, W.J., and Lockwood, D.N. (2004). Leprosy. Lancet *363*, 1209–1219.

Büeler, H., Aguzzi, A., Sailer, A., Greiner, R.A., Autenried, P., Aguet, M., and Weissmann, C. (1993). Mice devoid of PrP are resistant to scrapie. Cell *73*, 1339–1347.

Büeler, H., Fischer, M., Lang, Y., Bluethmann, H., Lipp, H.P., DeArmond, S.J., Prusiner, S.B., Aguet, M., and Weissmann, C. (1992). Normal development and behaviour of mice lacking the neuronal cell-surface PrP protein. Nature *356*, 577–582.

De Togni, P., Goellner, J., Ruddle, N.H., Streeter, P.R., Fick, A., Mariathasan, S., Smith, S.C., Carlson, R., Shornick, L.P., Strauss-Schoenberger, J., et al. (1994). Abnormal development of peripheral lymphoid organs in mice deficient in lymphotoxin. Science *264*, 703–707.

Dlakic, W.M., Grigg, E., and Bessen, R.A. (2007). Prion infection of muscle cells in vitro. J. Virol. *81*, 4615–4624.

Drayton, D.L., Liao, S., Mounzer, R.H., and Ruddle, N.H. (2006). Lymphoid organ development: From ontogeny to neogenesis. Nat. Immunol. *7*, 344–353.

Ernst, J.D., Trevejo-Nunez, G., and Banaiee, N. (2007). Genomics and the evolution, pathogenesis, and diagnosis of tuberculosis. J. Clin. Invest. *117*, 1738–1745.

Falsig, J., Julius, C., Margalith, I., Schwarz, P., Heppner, F.L., and Aguzzi, A. (2008). A versatile prion replication assay in organotypic brain slices. Nat. Neurosci. *11*, 109–117.

Fischer, M., Rülicke, T., Raeber, A., Sailer, A., Moser, M., Oesch, B., Brandner, S., Aguzzi, A., and Weissmann, C. (1996). Prion protein (PrP) with amino-proximal deletions restoring susceptibility of PrP knockout mice to scrapie. EMBO J. *15*, 1255–1264.

Fraser, H., and Dickinson, A.G. (1970). Pathogenesis of scrapie in the mouse: The role of the spleen. Nature *226*, 462–463.

Futterer, A., Mink, K., Luz, A., Kosco-Vilbois, M.H., and Pfeffer, K. (1998). The lymphotoxin beta receptor controls organogenesis and affinity maturation in peripheral lymphoid tissues. Immunity *9*, 59–70.

Glatzel, M., Abela, E., Maissen, M., and Aguzzi, A. (2003). Extraneural pathologic prion protein in sporadic Creutzfeldt-Jakob disease. N. Engl. J. Med. *349*, 1812–1820.

Hamir, A.N., Kunkle, R.A., Miller, J.M., and Hall, S.M. (2006). Abnormal prion protein in Ectopic lymphoid tissue in a kidney of an asymptomatic white-tailed deer experimentally inoculated with the agent of chronic wasting disease. Vet. Pathol. *43*, 367–369.

Hanayama, R., Tanaka, M., Miyasaka, K., Aozasa, K., Koike, M., Uchiyama, Y., and Nagata, S. (2004). Autoimmune disease and impaired uptake of apoptotic cells in MFG-E8-deficient mice. Science *304*, 1147–1150.

Heikenwalder, M., Zeller, N., Seeger, H., Prinz, M., Klohn, P.C., Schwarz, P., Ruddle, N.H., Weissmann, C., and Aguzzi, A. (2005). Chronic lymphocytic inflammation specifies the organ tropism of prions. Science *307*, 1107–1110.

Iannuzzi, M.C., Rybicki, B.A., and Teirstein, A.S. (2007). Sarcoidosis. N. Engl. J. Med. *357*, 2153–2165.

Kaeser, P.S., Klein, M.A., Schwarz, P., and Aguzzi, A. (2001). Efficient lymphoreticular prion propagation requires prp(c) in stromal and hematopoietic cells. J. Virol. *75*, 7097–7106.

Klein, M.A., Frigg, R., Flechsig, E., Raeber, A.J., Kalinke, U., Bluethmann, H., Bootz, F., Suter, M., Zinkernagel, R.M., and Aguzzi, A. (1997). A crucial role for B cells in neuroinvasive scrapie. Nature *390*, 687–690.

Klein, M.A., Frigg, R., Raeber, A.J., Flechsig, E., Hegyi, I., Zinkernagel, R.M., Weissmann, C., and Aguzzi, A. (1998). PrP expression in B lymphocytes is not required for prion neuroinvasion. Nat. Med. *4*, 1429–1433.

Klohn, P.C., Stoltze, L., Flechsig, E., Enari, M., and Weissmann, C. (2003). A quantitative, highly sensitive cell-based infectivity assay for mouse scrapie prions. Proc. Natl. Acad. Sci. USA *100*, 11666–11671.

Kovacs, G.G., Lindeck-Pozza, E., Chimelli, L., Araujo, A.Q., Gabbai, A.A., Strobel, T., Glatzel, M., Aguzzi, A., and Budka, H. (2004). Creutzfeldt-Jakob disease and inclusion body myositis. Ann. Neurol. *55*, 121–125.

Kranich, J., Krautler, N.J., Heinen, E., Polymenidou, M., Bridel, C., Schildknecht, A., Huber, C., Kosco-Vilbois, M.H., Zinkernagel, R., Miele, G., and Aguzzi, A. (2008). Follicular dendritic cells control engulfment of apoptotic bodies by secreting Mfge8. J. Exp. Med. *205*, 1293–1302.

Kumar, V., Abbas, A.K., Fausto, N., Robbins, S.L., and Cotran, R.S. (2004). Robbins and Cotran Pathologic Basis of Disease (Amsterdam: Elsevier Science).

Legname, G., Baskakov, I.V., Nguyen, H.O., Riesner, D., Cohen, F.E., DeArmond, S.J., and Prusiner, S.B. (2004). Synthetic mammalian prions. Science *305*, 673–676.

Ligios, C., Sigurdson, C.J., Santucciu, C., Carcassola, G., Manco, G., Basagni, M., Maestrale, C., Cancedda, M.G., Madau, L., and Aguzzi, A. (2005). PrP(Sc) in mammary glands of sheep affected by scrapie and mastitis. Nat. Med. *11*, 1137–1138.

Link, A., Vogt, T.K., Favre, S., Britschgi, M.R., Acha-Orbea, H., Hinz, B., Cyster, J.G., and Luther, S.A. (2007). Fibroblastic reticular cells in lymph nodes regulate the homeostasis of naive T cells. Nat. Immunol. *8*, 1255–1265.

Mabbott, N.A., Mackay, F., Minns, F., and Bruce, M.E. (2000). Temporary inactivation of follicular dendritic cells delays neuroinvasion of scrapie. Nat. Med. *6*, 719–720.

Mabbott, N.A., McGovern, G., Jeffrey, M., and Bruce, M.E. (2002). Temporary blockade of the tumor necrosis factor receptor signaling pathway impedes the spread of scrapie to the brain. J. Virol. *76*, 5131–5139.

Mabbott, N.A., Young, J., McConnell, I., and Bruce, M.E. (2003). Follicular dendritic cell dedifferentiation by treatment with an inhibitor of the lymphotoxin pathway dramatically reduces scrapie susceptibility. J. Virol. *77*, 6845–6854.

Mackay, F., and Browning, J.L. (1998). Turning off follicular dendritic cells. Nature *395*, 26–27.

Mackay, F., Majeau, G.R., Lawton, P., Hochman, P.S., and Browning, J.L. (1997). Lymphotoxin but not tumor necrosis factor functions to maintain splenic architecture and humoral responsiveness in adult mice. Eur. J. Immunol. *27*, 2033–2042.

Mahal, S.P., Baker, C.A., Demczyk, C.A., Smith, E.W., Julius, C., and Weissmann, C. (2007). Prion strain discrimination in cell culture: The cell panel assay. Proc. Natl. Acad. Sci. USA *104*, 20908–20913.

Mathiason, C.K., Powers, J.G., Dahmes, S.J., Osborn, D.A., Miller, K.V., Warren, R.J., Mason, G.L., Hays, S.A., Hayes-Klug, J., Seelig, D.M., et al. (2006). Infectious prions in the saliva and blood of deer with chronic wasting disease. Science *314*, 133–136.

Montrasio, F., Cozzio, A., Flechsig, E., Rossi, D., Klein, M.A., Rulicke, T., Raeber, A.J., Vosshenrich, C.A., Proft, J., Aguzzi, A., and Weissmann, C. (2001). B lymphocyte-restricted expression of prion protein does not enable prion replication in prion protein knockout mice. Proc. Natl. Acad. Sci. USA *98*, 4034–4037.

Montrasio, F., Frigg, R., Glatzel, M., Klein, M.A., Mackay, F., Aguzzi, A., and Weissmann, C. (2000). Impaired prion replication in spleens of mice lacking functional follicular dendritic cells. Science *288*, 1257–1259.

Moore, R.C., Redhead, N.J., Selfridge, J., Hope, J., Manson, J.C., and Melton, D.W. (1995). Double replacement gene targeting for the production of a series of mouse strains with different prion protein gene alterations. Biotechnology (N. Y.) *13*, 999–1004.

Okabe, M., Ikawa, M., Kominami, K., Nakanishi, T., and Nishimune, Y. (1997). Green mice as a source of ubiquitous green cells. FEBS Lett. *407*, 313–319.

Oldstone, M.B., Race, R., Thomas, D., Lewicki, H., Homann, D., Smelt, S., Holz, A., Koni, P., Lo, D., Chesebro, B., and Flavell, R. (2002). Lymphotoxin-alpha- and lymphotoxin-beta-deficient mice differ in susceptibility to scrapie: Evidence against dendritic cell involvement in neuroinvasion. J. Virol. *76*, 4357–4363.

Ordway, D., Henao-Tamayo, M., Orme, I.M., and Gonzalez-Juarrero, M. (2005). Foamy macrophages within lung granulomas of mice infected with Mycobacterium tuberculosis express molecules characteristic of dendritic cells and antiapoptotic markers of the TNF receptor-associated factor family. J. Immunol. *175*, 3873–3881.

Polymenidou, M., Stoeck, K., Glatzel, M., Vey, M., Bellon, A., and Aguzzi, A. (2005). Coexistence of multiple PrPSc types in individuals with Creutzfeldt-Jakob disease. Lancet Neurol. *4*, 805–814.

Priller, J., Prinz, M., Heikenwalder, M., Zeller, N., Schwarz, P., and Aguzzi, A. (2006). Early and rapid engraftment of bone marrow-derived microglia in scrapie. J. Neurosci. *26*, 11753–11762.

Prinz, M., Heikenwalder, M., Junt, T., Schwarz, P., Glatzel, M., Heppner, F.L., Fu, Y.X., Lipp, M., and Aguzzi, A. (2003). Positioning of follicular dendritic cells within the spleen controls prion neuroinvasion. Nature *425*, 957–962.

Prinz, M., Montrasio, F., Klein, M.A., Schwarz, P., Priller, J., Odermatt, B., Pfeffer, K., and Aguzzi, A. (2002). Lymph nodal prion replication and neuroinvasion in mice devoid of follicular dendritic cells. Proc. Natl. Acad. Sci. USA *99*, 919–924.

Prusiner, S.B., Cochran, S.P., Groth, D.F., Downey, D.E., Bowman, K.A., and Martinez, H.M. (1982). Measurement of the scrapie agent using an incubation time interval assay. Ann. Neurol. *11*, 353–358.

Russell, D.G. (2007). Who puts the tubercle in tuberculosis? Nat. Rev. Microbiol. *5*, 39–47.

Scandella, E., Bolinger, B., Lattmann, E., Miller, S., Favre, S., Littman, D.R., Finke, D., Luther, S.A., Junt, T., and Ludewig, B. (2008). Restoration of lymphoid organ integrity through the interaction of lymphoid tissue-inducer cells with stroma of the T cell zone. Nat. Immunol. *9*, 667–675.

Seeger, H., Heikenwalder, M., Zeller, N., Kranich, J., Schwarz, P., Gaspert, A., Seifert, B., Miele, G., and Aguzzi, A. (2005). Coincident scrapie infection and nephritis lead to urinary prion excretion. Science *310*, 324–326.

Selfridge, J., Pow, A.M., McWhir, J., Magin, T.M., and Melton, D.W. (1992). Gene targeting using a mouse HPRT minigene/HPRT-deficient embryonic stem cell system: Inactivation of the mouse ERCC-1 gene. Somat. Cell Mol. Genet. *18*, 325–336.

Taraboulos, A., Jendroska, K., Serban, D., Yang, S.L., DeArmond, S.J., and Prusiner, S.B. (1992). Regional mapping of prion proteins in brain. Proc. Natl. Acad. Sci. USA *89*, 7620–7624.

Thomzig, A., Schulz-Schaeffer, W., Wrede, A., Wemheuer, W., Brenig, B., Kratzel, C., Lemmer, K., and Beekes, M. (2007). Accumulation of pathological prion protein PrPSc in the skin of animals with experimental and natural scrapie. PLoS Pathog. *3*, e66.

Vascellari, M., Nonno, R., Mutinelli, F., Bigolaro, M., Di Bari, M.A., Melchiotti, E., Marcon, S., D'Agostino, C., Vaccari, G., Conte, M., et al. (2007). PrPSc in Salivary Glands of Scrapie-Affected Sheep. J. Virol. *81*, 4872–4876.

Vorberg, I., Buschmann, A., Harmeyer, S., Saalmüller, A., Pfaff, E., and Groschup, M.H. (1999). A novel epitope for the specific detection of exogenous prion proteins in transgenic mice and transfected murine cell lines. Virology *255*, 26–31.

Vorberg, I., Raines, A., Story, B., and Priola, S.A. (2004). Susceptibility of common fibroblast cell lines to transmissible spongiform encephalopathy agents. J. Infect. Dis. *189*, 431–439.